The Abdus Salam
International Centre for Theoretical Physics

United Nations
Educational, Scientific and
Cultural Organization

IAEA
International Atomic Energy Agency

1859-32

Summer School on Novel Quantum Phases and Non-Equilibrium Phenomena in Cold Atomic Gases

27 August - 7 September, 2007

Fundamentals of spinor Bose-Einstein Condensates

Masahito Ueda
Tokyo Institute of Technology

Fundamentals of Spinor Bose-Einstein Condensates

Masahito UEDA

Tokyo Institute of Technology,
ERATO, JST

Collaborators

Yuki Kawaguchi (Tokyo Institute of Technology)

Hiroki Saito (University of Electro-Communications)

Contents

- Comparing atomic-gas BEC with superfluid helium
  → Where to look for phenomena unique to atomic-gas BEC?
- Basics of spinor BEC physics
  - ground-state phase diagram
  - many-body effects
  - topological excitations
- Some more recent topics
  - spin vortex
  - quench dynamics

Atomic-gas BEC vs. Superfluid Helium

Atomic gases and helium both exhibit BEC and superfluidity,
but at the same time they show striking complementarity in

- kinetics,
- magnetism, and
- symmetry breaking.

How different are they in these respects?

	Superfluid helium	Atomic-gas BEC
Kinetics	collision time collective mode $\tau_{\mathrm{col}} \sim 10^{-12}\,\mathrm{s} \ll \omega^{-1}$ ⬇ • local equilibrium achieved • physics can be understood by conservation laws (energy, continuity equation, etc.) and hydrodynamics, even thought the system is strongly interacting.	$\tau_{\mathrm{col}} \sim 10^{-3}\,\mathrm{s} \sim \omega^{-1}$ ⬇ • local equilibrium not achieved • nonequilibrium relaxation and kinetics essential for understanding BEC phase transition and vortex nucleation 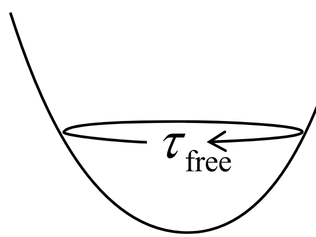 $\tau_{\mathrm{free}} < \tau_{\mathrm{col}}$
Magnetism	nuclear spin (^{3}He)	• alkalis: electronic spin : $\mu_e \approx 2000\mu_N$ →allow control the spin texture locally • new quantum phases such as cyclic phase emerge in high-spin systems
Symmetry breaking	• bulk He: thermodynamic limit achieved • spontaneous symmetry breaking of the relative gauge (phase) ⬇ emergence of the mean field	mesoscopic (not thermodynamic limit) ⬇ • symmetry breaking may or may not occur • dynamics of symmetry breaking can be observed due to long collision time

Local Manipulation of Spin Textures

A. E. Leanhardt, et al., Phys. Rev. Lett. **90**, 140403 (2003)

total density
coreless vortex

density profiles of
individual spin
components

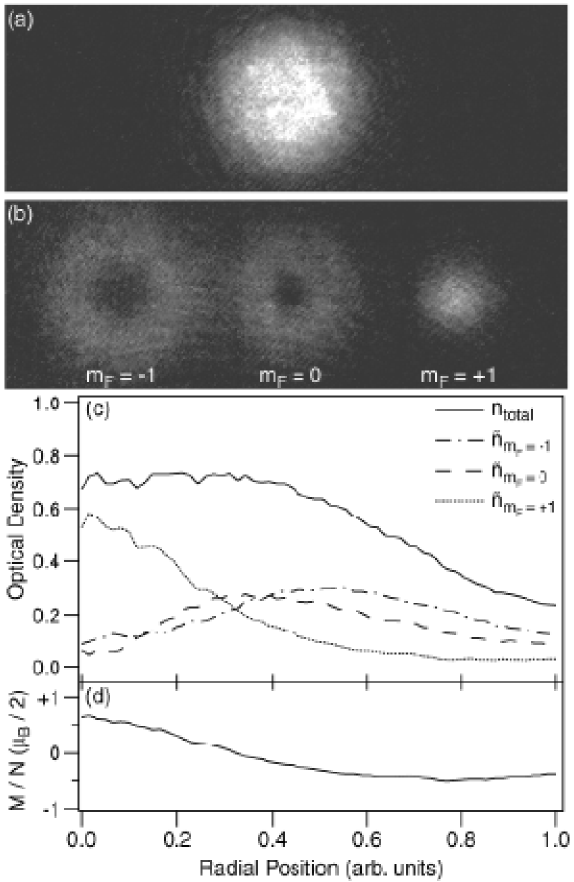

spin-1 ^{23}Na condensate
topological phase imprinting using
quadrupole magnetic field

$$\mathbf{B}(\mathrm{r},\ \phi,\ \mathrm{z}) = \mathrm{B_z}\hat{\mathrm{z}} + \mathrm{B'r}\left(\cos(2\phi)\hat{\mathrm{r}} - \sin(2\phi)\hat{\phi}\right)$$

$$\mathrm{B_z} \to 0$$

$$\left|\zeta(\mathrm{r},\phi,\mathrm{z})\right\rangle = e^{2i\phi}\cos^2\frac{\beta(r)}{2}\left|1,-1\right\rangle - e^{i\phi}\frac{\sin\beta(r)}{\sqrt{2}}\left|1,\ 0\right\rangle + \sin^2\frac{\beta(r)}{2}\left|1,\ +1\right\rangle$$

$\beta(0) = 0,\quad \beta(\infty) = \pi$ (skyrmion)

$= \dfrac{\pi}{2}$ (meron)

The local spin texture has thus been manipulated by external magnetic field.

Basics of spinor BEC physics

Internal Degrees of Freedom: Hyperfine Spin F

- Alkali atoms have electronic and nuclear spins.

			hyperfine spin
electronic spin	$S=\frac{1}{2}$		
nuclear spin	$I=\frac{1}{2}$	$^{1}\mathrm{H}$	$(F=1,0)$
	$\frac{3}{2}$	$^{23}\mathrm{Na}$, $^{39}\mathrm{K}$, $^{87}\mathrm{Rb}$	$(F=1,2)$
	$\frac{5}{2}$	$^{85}\mathrm{Rb}$	$(F=2,3)$
	$\frac{7}{2}$	$^{133}\mathrm{Cs}$	$(F=3,4)$

- Hyperfine interaction $V = AS \cdot I$

$$\Delta E_{\mathrm{hf}} = V\big|_{F=I+\frac{1}{2}} - V\big|_{F=I-\frac{1}{2}} \sim \text{a few GHz} \sim 0.1\mathrm{K} \gg k_{\mathrm{B}}T \text{ for BEC}$$

Therefore the hyperfinr spin $\boldsymbol{F}=\boldsymbol{S}+\boldsymbol{I}$ is a good quantum number.

$\longrightarrow$ Several spin states are available in BECs.

Novel quantum phases emerge for high-spin BECs.

Spinor BEC in an Optical Trap

- In a magnetic trap, the spin of each atom is fixed by local magnetic field, so that the internal degrees of freedom are frozen.
  →The order parameter is scalar.

- In an optical trap, the atomic states for a given F are degenerate with respect to magnetic quantum number $m_F = F,\ F-1,\ \ldots\ldots,\ -F$
  →The order parameter is a spherical tensor of rank F

$$\psi_m\left(m = F,\ F-1, \ldots, -F\right)$$

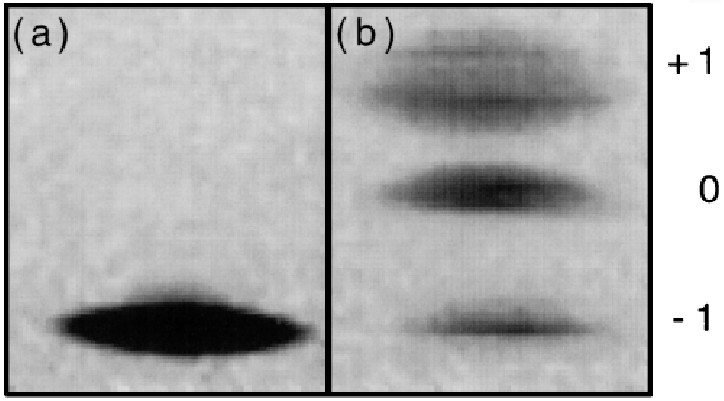

D. Stamper-Kurn, et.al., Phys. Rev. Lett. **80**, 2027 (1998)

- A rich variety of order-parameter manifolds are available, depending on the value of F.

F=1 FM BEC $\quad \mathrm{SO}(3)$ (continuous spin-gauge symmetry)

F=1 AFM BEC $\quad \dfrac{\mathrm{U}(1)\times \mathrm{S}^2}{\mathrm{Z}_2}$ (discreate spin-gauge symmetry)

→ These symmetries of the order paramters are reflected in the nature of Goldstone modes, spin textures, and topological excitations.

Mean Field Theory of Spin-1 BECs

T.Ohmi and K.Machida, J. Phys. Soc. Jpn. **67**, 1822 (1998)
T.-L.Ho, Phys. Rev. Lett. **81**, 742 (1998)

$$E=\int d\mathbf{r}\left(\underbrace{\sum_m \frac{\hbar^2}{2M}\left|\nabla\psi_m\right|^2}_{\text{kinetic}}+\underbrace{\sum_m U_{\text{trap}}\left|\psi_m\right|^2}_{\text{one-body potential}}+\underbrace{\frac{g_0+2g_2}{6}n^2}_{\text{Hartree}}+\underbrace{\frac{g_2-g_0}{6}n^2\left|\langle\mathbf{F}\rangle\right|^2}_{\text{spin-exchange}}\right)$$

$$n=\sum_m\left|\psi_m\right|^2,\quad \underbrace{\langle\mathbf{F}\rangle=\frac{1}{n}\sum_{m,n}\psi_m^*\mathbf{F}_{mn}\psi_n}_{\text{local spin density}}$$

$$g_i=\frac{4\pi\hbar^2}{m}a_i\quad(i=0,2)$$

(a) $g_2<g_0$: ferromagnetic

Euler angles α, β, γ

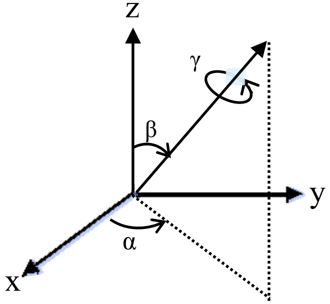

$$\left|\langle\mathbf{F}\rangle\right|=1\rightarrow\begin{pmatrix}\psi_1\\\psi_0\\\psi_{-1}\end{pmatrix}=\sqrt{n}\begin{pmatrix}1\\0\\0\end{pmatrix}$$

In general,

$$\hat{U}(\alpha,\beta,\gamma)=e^{-i\hat{F}_z\alpha}e^{-i\hat{F}_y\beta}e^{-i\hat{F}_z\gamma}$$

spin-gauge symmetry

gauge rotation

$$\begin{pmatrix}\psi_1\\\psi_0\\\psi_{-1}\end{pmatrix}=e^{i\phi}\sqrt{n}\,\hat{U}(\alpha,\beta,\gamma)\begin{pmatrix}1\\0\\0\end{pmatrix}=e^{i(\phi-\gamma)}\sqrt{n}\begin{pmatrix}e^{-i\alpha}\cos^2\frac{\beta}{2}\\\frac{1}{\sqrt{2}}\sin\beta\\e^{i\alpha}\sin^2\frac{\beta}{2}\end{pmatrix}$$

Gauge angle φ and rotation angle γ appear as φ-γ.
This continuous spin-gauge symmetry allows the system to have coreless vortex
texture-induced supercurrent .

order –parameter manifold SO(3)

(b) $g_2>g_0$: antiferromagnetic or polar

$$\left|\langle\mathbf{F}\rangle\right|=0\rightarrow\begin{pmatrix}\psi_1\\\psi_0\\\psi_{-1}\end{pmatrix}=\sqrt{\frac{n}{2}}\begin{pmatrix}1\\0\\1\end{pmatrix}\quad\text{or}\quad\sqrt{n}\begin{pmatrix}0\\1\\0\end{pmatrix}$$

In general,

$$\begin{pmatrix}\psi_1\\\psi_0\\\psi_{-1}\end{pmatrix}=e^{i\phi}\sqrt{\mathrm{n}}\,\hat{U}(\alpha,\beta,\gamma)\begin{pmatrix}0\\1\\0\end{pmatrix}=e^{i\phi}\sqrt{\frac{\mathrm{n}}{2}}\begin{pmatrix}-e^{-i\alpha}\sin\beta\\\sqrt{2}\cos\beta\\e^{i\alpha}\sin\beta\end{pmatrix}$$

The order parameter is invariant under simultaneous β→π-β & φ→φ+π.
This discrete spin-gauge symmetry allows the system to hold a 1/2 vortex.

order-parameter manifold $\dfrac{U(1)\times S^2}{Z_2}$

F. Zhou, Phys. Rev. Lett. **87**, 80401 (2001)

Many-Body Gound State of a Spin-1 BEC

Law, et al., Phys. Rev. Lett. **81**, 5257 (1988)
Koashi and MU, Phys. Rev. Lett. **84**,1066 (2000)
Ho and Yip, Phys. Rev. Lett. **84**, 4031 (2000)

$1 \otimes 1 = 2 \oplus 0 \oplus 1$

forbidden by Bose symmetry

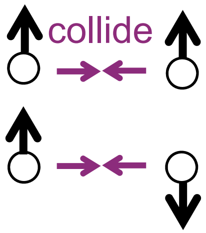

total spin 2: scattering length a_2

total spin 0: scattering length a_0

$a_2 < a_0$

$\uparrow\uparrow\uparrow\cdots\cdots\uparrow$ Bose ferromagnet $\left|\mathrm{BEC}\right\rangle = \frac{1}{\sqrt{N!}}\left(\hat{a}_1^\dagger\right)^N \left|\mathrm{vac}\right\rangle$

$a_2 > a_0$

Spin-singlet correlation $\uparrow\downarrow$ is favored. Bose antiferromagnet with no Neel order

$$\hat{S}^\dagger = \frac{1}{\sqrt{3}}\left(\hat{a}_0^{\dagger 2} - 2\hat{a}_1^\dagger \hat{a}_{-1}^\dagger\right) \qquad \left|\mathrm{BEC}\right\rangle \sim \left(\hat{S}^\dagger\right)^{\frac{N}{2}} \left|\mathrm{vac}\right\rangle \to \text{symmetry } \mathrm{U}(1) \qquad n_1 = n_0 = n_{-1} = \frac{N}{3}$$

cf. mean field: $\psi = \sum_{m=-1}^{1} a_m Y_1^m \cdots \frac{U(1)\times S^2}{Z_2}$ $\quad n_0 = 0$ $\rightarrow$ How can this discrepancy be reconciled ?

Connection between Many-Body Theory and Mean-Field Theory

In fact, mean-field theory breaks down at zero magnetic field, but its validity is quickly restored as the magnetic field increases.

Suppose that all bosons form spin-singlet pairs and all magnetic sublevels are equally populated.

$$|\mathrm{BEC}\rangle \sim \left(\hat{a}_0^{\dagger 2} - 2\hat{a}_1^{\dagger}\hat{a}_{-1}^{\dagger}\right)^{\frac{N}{2}} |\mathrm{vac}\rangle \;\rightarrow\; n_1 = n_0 = n_{-1} = \frac{N}{3}$$

As the magnetic field increases, singlet pairs are broken one by one via spin flip: ⇅ → ⇈.

Connection between Many-Body Theory and Mean-Field Theory

When m pairs are broken, the many-body state becomes

$$\left(\hat{S}^\dagger\right)^{\frac{N}{2}} |\mathrm{vac}>$$

↓ spin flip of m singlet pairs

$$\left(\hat{a}_1^\dagger\right)^{2m}\left(\hat{S}^\dagger\right)^{\frac{N}{2}-m} |\mathrm{vac}\rangle \qquad \hat{S}^\dagger = \frac{1}{\sqrt{3}}\left(\hat{a}_0^{\dagger 2} - 2\hat{a}_1^\dagger \hat{a}_{-1}^\dagger\right)$$

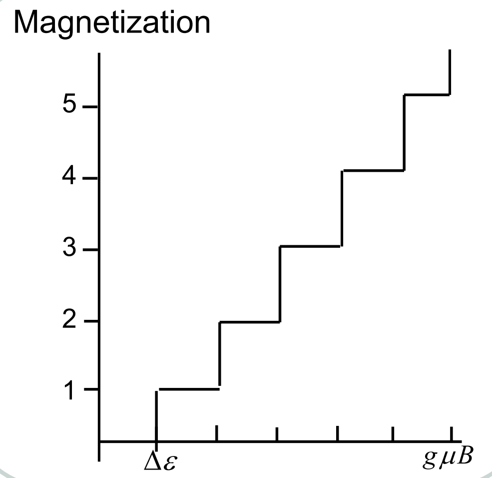

Each time a spin-singlet pair is broken, the m=0 component is exponentially suppressed due to *inverse* bosonic enhancement effect $\left(\hat{a}^\dagger |n\rangle = \sqrt{n+1}|n+1>\right)$.

The m =0 component virtually disappears at $m \sim N^{1/2}$, beyond which mean field theory is restored.

The fractional dependence on *N* indicates that the manybody effect can appear in the mesoscopic regime.

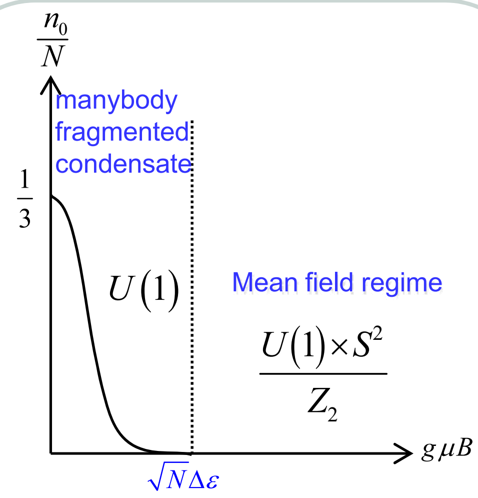

M. Koashi & MU, Phys. Rev. Lett. **84** 1066 (2000)

Spin-2 BEC

$$2\otimes 2 = 0\oplus 2\oplus 4\underbrace{\oplus 1\oplus 3}$$

a_0 a_2 a_4 forbidden by Bose symmetry

Koashi & MU, Phys. Rev. Lett. **84**, 1066 (2000)
Ciobanu, et al., Phys. Rev. A **61**,033607 (2000)
MU & Koashi., Phys. Rev. A **65**, 063602 (2002)

Interaction Hamiltonian

$$\hat{V} = \frac{1}{2}\int d\mathbf{r}\left[c_0 :\hat{n}^2: + c_1 :\hat{\mathbf{F}}^2: + c_2 \hat{S}^\dagger \hat{S}\right]$$

$$c_0 = \frac{4\pi\hbar^2}{M}\frac{4a_2+3a_4}{7}$$
$$c_1 = \frac{4\pi\hbar^2}{M}\frac{a_4-a_2}{7}$$
$$c_2 = \frac{4\pi\hbar^2}{M}\frac{7a_0-10a_2+3a_4}{7}$$

$\hat{n} = \sum_m \hat{\psi}_m^\dagger \hat{\psi}_m$ … particle density

$\hat{\mathbf{F}} = \sum_m \hat{\psi}_m^\dagger \mathbf{f}_{mn} \hat{\psi}_n$ … spin density

$\hat{S} = \sum_m \frac{(-1)^m}{\sqrt{5}} \hat{\psi}_m \hat{\psi}_{-m}$ … spin-singlet pair amplitude

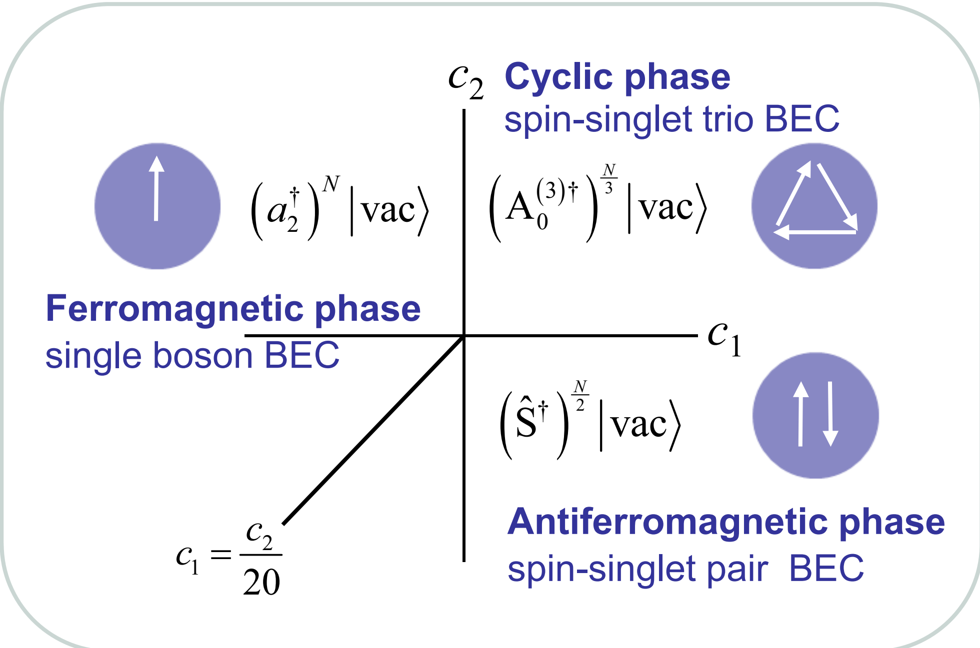

The pairwise and trio-wise units bring about some unique features of spin-2 BEC.

" Meissner Effect " of the Antiferromagnetic Spin-2 BEC

Minimize the spin-dependent part of the Hamiltonian

$$\hat{H}^{\rm spin} = \frac{c_1}{2V^{\rm eff}} : \hat{\mathbf{F}}^2 : + \frac{2c_2}{5V^{\rm eff}} \hat{S}^\dagger \hat{S} - \underbrace{p\hat{F}_z}_{\text{Zeeman term}} \qquad p = g\mu B \qquad |N, N_s, F, F_z; \lambda\rangle$$

\# of trio singlets (λ)

\# of spin-single pairs (N_s)

with respect to magnetization F_z :

This term counteracts B because $c_2 < 0$.

$$E(F_z, l) = \frac{c_1'}{2V^{\rm eff}} \left[F_z - \frac{g\mu V^{\rm eff}}{c_1'} \left(B + \frac{c_2}{8g\mu V^{\rm eff}} \right) + \frac{1}{2} \right]^2 - \frac{c_2}{40V^{\rm eff}} l(l + 2F + 6) + \text{const.}$$

$$l = 2(N - 2N_s) - F_z$$

$$c_1' \equiv \frac{1}{V^{\rm eff}} \left(c_1 - \frac{c_2}{20} \right) > 0$$

$$c_2 < 0 \quad \text{for AFM}$$

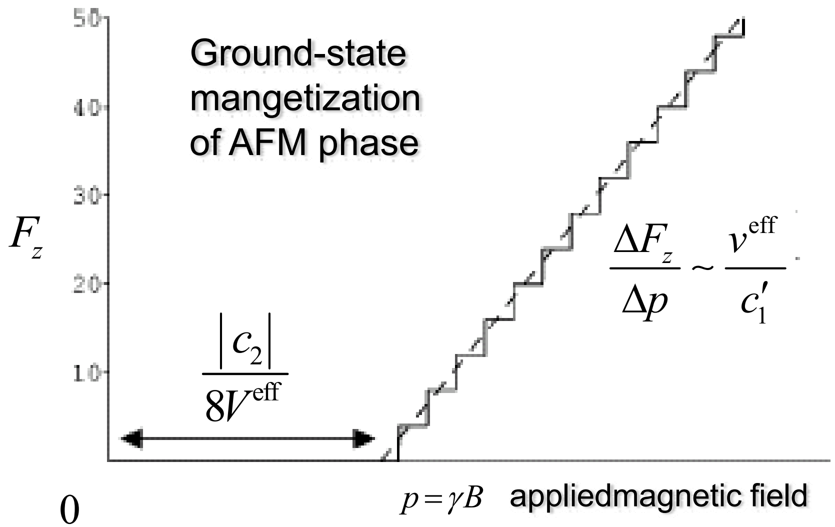

Physically, the $F=2$ spin-singlet pair condensate acts to screen the external magnetic field until the magnetic field reaches a critical value.

↓

$B^{\rm critical} \sim 1/V^{\rm eff}$

mesoscopic Meissner effect

MU & M. Koashi, Phys. Rev. A **65**, 063602 (2002)

Spinor BECs can hold various topological excitations.

Fractional Vortices

F=1 polar (*pair singlet*)

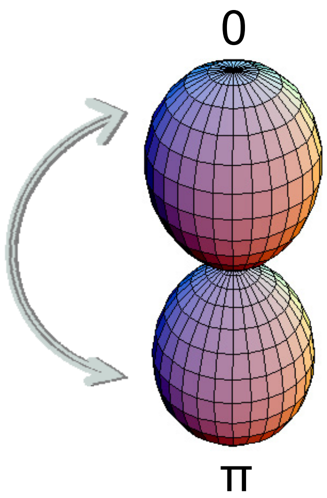

$\psi \propto e^{i\phi}\cos\theta$

two-fold symmetry

The order parameter invariant under

$\theta \to \pi - \theta$ (spatial inversion)

$\phi \to \phi + \pi$ (gauge transformation)

1/2 vortex

cf. no 1/2 vortex for F=2 AF BEC

F. Zhou, Phys. Rev. Lett. **87**, 080401 (2001)

F=2 cyclic (*trio singlet*)

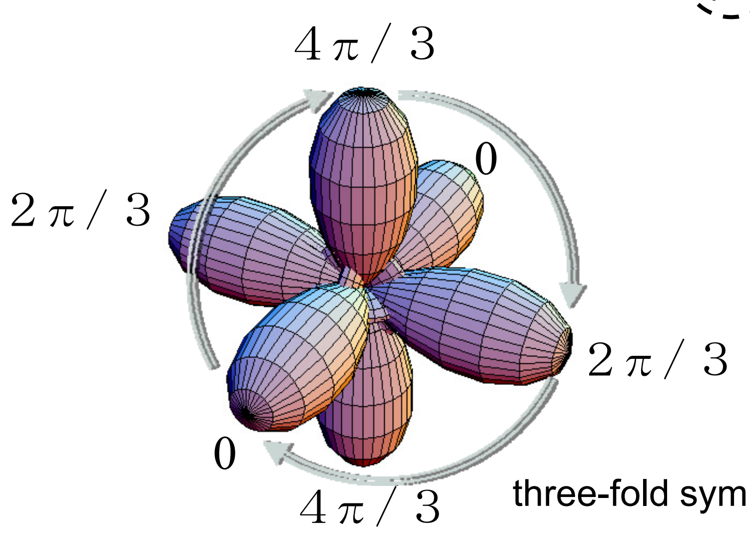

three-fold symmetry

invariant under

$2\pi/3$ rotation about n=(1,1,1)

$\phi \to \phi + 2\pi/3$

1/3 vortex

Y. Zhang, et. al. cond-mat/0404138

H. Mäkelä, J. Phys. A: Math Gen. **39**, 7423 (2006)

G. W. Semenoff and F. Zhou, Phys. Rev. Lett. **98**, 100401 (2007)

Fragmentation of BEC

What's BEC?

The system exhibits BEC when the largest eigenvalue of the one-particle reduced density matrix is an extensive rather than an intensive quantity.

O. Penrose & L. Onsager, Phys. Rev. **104**, 576 (1956)

Is the number of extensive eigenvalues necessarily one?
If there is more than one such eigenvalue, the BEC is said to be fragmented.

P. Nozieres and D. Saint James, J. Physique **43**, 1133 (1982)

Three Conditions for Fragmented BEC

- The system must have exact symmetry that allows degeneracy.
- The interaction between the degenerate states must be attractive to gain the Fock exchange energy
- The system must be mesoscopic to avoid collapse or symmetry breaking into a single BEC

classic examples

rotating BEC with attractive interaction in a harmonic trap

N. Wilkin, J. Gunn & R. Smith, Phys. Rev. Lett. **80**, 2265 (1998)

antiferromagnetic BEC — "effective" attractive interaction (i.e., $a_2 > a_0 > 0$) in the spin-singlet channel

T. -L. Ho and S. K. Yip, Phys. Rev. Lett. **84**, 4031 (2000)
M. Koashi and MU, Phys. Rev. Lett. **84**, 1066 (2000)

Why is the fragmented BEC so difficult to observe in reality?

The fragmented BEC is very fragile against symmetry-breaking perturbations.

Fragmented BEC fragile against symmetry-breaking perturbation

E. Mueller, et al., Phys. Rev. A **74**, 33612 (2006)

example 1.

$$\left|\frac{N}{2}\right\rangle_1 \left|\frac{N}{2}\right\rangle_2 = \int_0^{2\pi} \frac{d\phi}{2\pi} \frac{1}{\sqrt{2^N N!}} \left(e^{i\phi}\hat{c}_1^\dagger + e^{-i\phi}\hat{c}_2^\dagger\right)^N |\mathrm{vac}\rangle$$

$\hat{H} = t\hat{c}_1^\dagger \hat{c}_2 + \text{h.c.}$ symmetry-breaking per turbation

matrix element $\propto t\sqrt{N_1 N_2} \propto t\,N$ (extensive) for $N_1 = N_2 = N/2$

$$\left|\frac{N}{2}\right\rangle_1 \left|\frac{N}{2}\right\rangle_2 \longrightarrow \frac{1}{\sqrt{2^N N!}} (e^{i\phi}\hat{c}_1^\dagger + e^{-i\phi}\hat{c}_2^\dagger)^N |\mathrm{vac}\rangle$$

example 2. (antiferromagnetic BEC)

$$|S=0\rangle \propto \left(\hat{\mathbf{A}}^\dagger \cdot \hat{\mathbf{A}}^\dagger\right)^{\frac{N}{2}} |\mathrm{vac}\rangle \propto \int \frac{d\,\mathbf{n}}{4\pi} \left(\mathbf{n}\cdot\hat{\mathbf{A}}^\dagger\right)^N |\mathrm{vac}\rangle \quad \hat{\mathrm{A}}_\mathrm{x} = -\frac{\hat{a}_1 + \hat{a}_{-1}}{\sqrt{2}},\ \hat{\mathrm{A}}_\mathrm{y} = \frac{\hat{a}_1 - \hat{a}_{-1}}{i\sqrt{2}},\ \mathrm{A}_\mathrm{z} = \hat{a}_0$$

This fragmented BEC is fragile against magnetic field because of bosonic stimulation.

Topological Defect Formation in Quenched Spinor BEC

Quench=rapid change in external parameters such as magnetic field

Topological Defect Formation in Quenched Ferromagnetic BEC

H. Saito, Y. Kawaguchi, MU, Phys. Rev. A**75**, 013621 (2007)

Phase diagram of spin-1 FM BEC

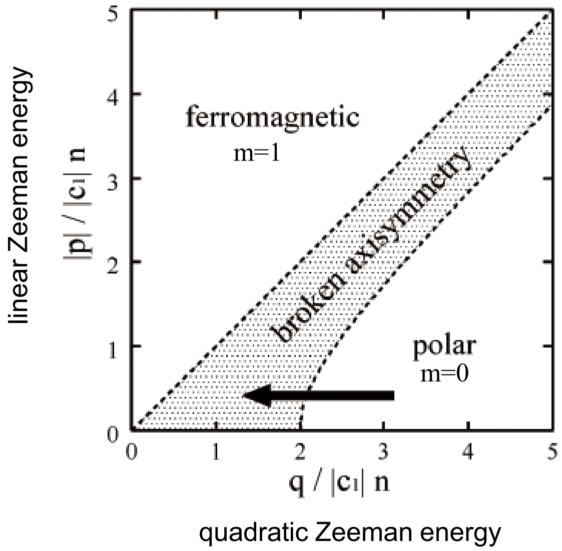

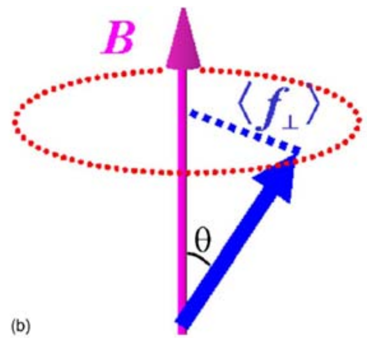

What happens to the BEC if we quench the B-field from the polar to the broken-axisymmetric phase?

The AM conservation prohibits a uniform magnetization.

K. Murata, et al., Phys. Rev. A 75, 013607 (2007)

Bogoliubov Spectrum of a Ferromagnetic BEC

H.Saito, Y.Kawaguchi, and M.U., Phys. Rev. Lett. **96**, 065302 (2006)

Suppose that all atoms are prepared in the $m=0$ state in a pancake-shaped trap.

In the $\leftrightarrow$ region the modes with orbital angular momentum $l=\pm 1$ have imaginary parts; they are therefore dynamically unstable and grow exponentially.

Bogoliubov spectrum for $l=0, \pm 1$ as a function of the spin-exchange interaction g_1^{2D}

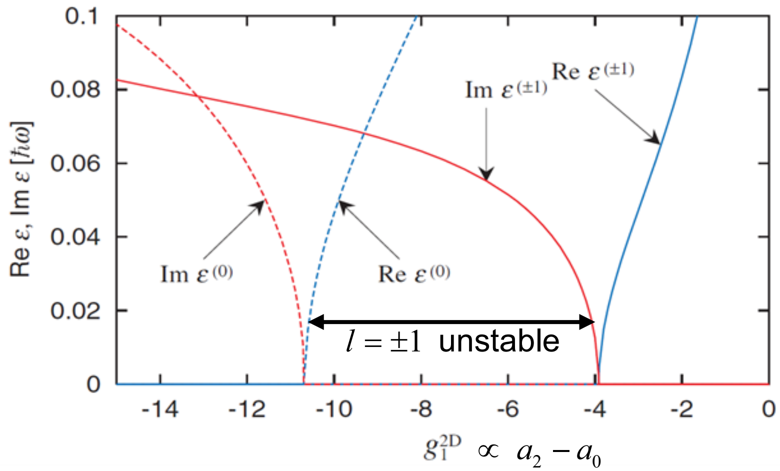

FIG. 1 (color). Real and imaginary parts of the lowest Bogoliubov energies $\varepsilon^{(\ell)}$ for $\ell = 0, \pm 1$, where the $m = \pm 1$ components of the eigenfunction are proportional to $e^{\pm i\ell\phi}$. The two energies $\varepsilon^{(\pm 1)}$ are degenerate due to the axisymmetry of the system. We have taken the parameters of spin-1 ^{87}Rb atoms, where the spin-independent interaction strength g_0^{2D} is related to the spin-dependent strength g_1^{2D} by $g_0^{2D} = -216.1 g_1^{2D}$.

Bogoliubov Spectrum of a Ferromagnetic BEC

H.Saito, Y.Kawaguchi, and M.U., Phys. Rev. Lett. **96**, 065302 (2006)

Bogoliubov spectrum for $l = 0, \pm 1$ as a function of the spin-exchange interaction g_1^{2D}

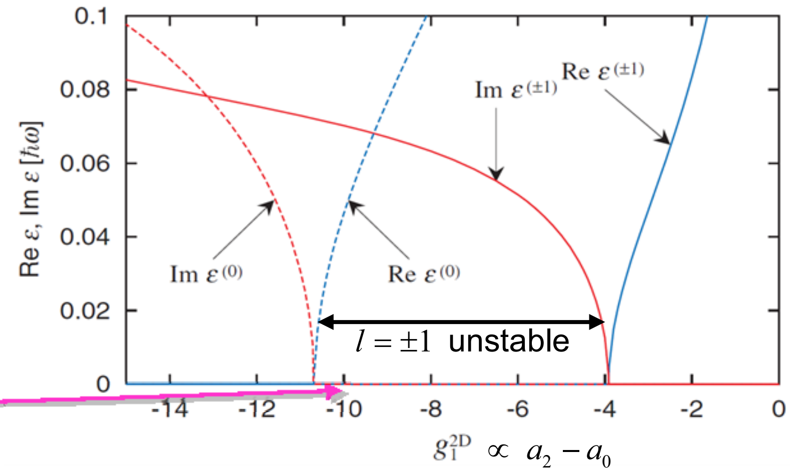

Suppose that the parameter of ^{87}Rb BEC is prepared at this point.

Then the system has orbital AM instability.

Prediction: the $l = \pm 1$ modes will start to grow and rotate spontaneously!

Chiral Symmetry in a Ferromagnetic BEC

The angular momentum conservation implies that the *l* =1 and *l* = -1 modes must be created simultaneously by the same amount.

There are two possibilities:

spin texture

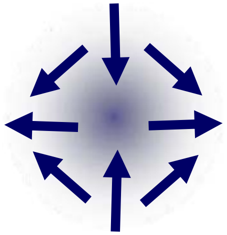

spin	orbital
$m=1$	$l=1$
$m=-1$	$l=-1$

degenerate

spin	orbital
$m=1$	$l=-1$
$m=-1$	$l=1$

spin texture

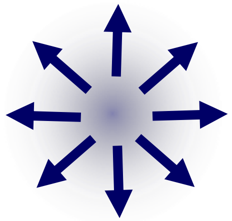

$$\psi_1 \propto e^{\pm i\phi} \qquad F_+ = F_x + iF_y = \sqrt{2}\left(\psi_1^* \psi_0 + \psi_0^* \psi_{-1}\right) \propto e^{\mp i\phi}$$

$$\psi_0 \propto 1 \qquad F_x \propto \cos\phi$$

$$\psi_{-1} \propto e^{\mp i\phi} \qquad F_y \propto \mp \sin\phi$$

Chiral Symmetry in a Ferromagnetic BEC

The angular momentum conservation implies that the *l* =1 and *l* = -1 modes must be created simultaneously by the same amount.

There are two possibilities:

spin texture

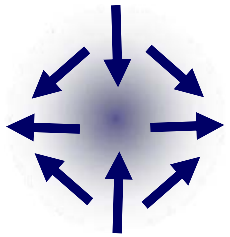

spin	orbital
$m=1$	$l=1$
$m=-1$	$l=-1$

degenerate

spin	orbital
$m=1$	$l=-1$
$m=-1$	$l=1$

spin texture

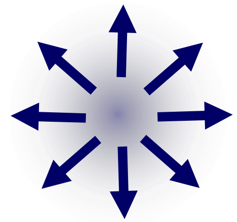

These two possibilities are degenerate, this degeneracy being a statement of the chiral symmetry.

Chiral Symmetry Breaking in a Ferromagnetic BEC

The chirally symmetric state lies higher in energy than the chiral-symmetry broken states.

Therefore the chiral symmetry will be dynamically broken and each spin component will begin to rotate spontaneously.

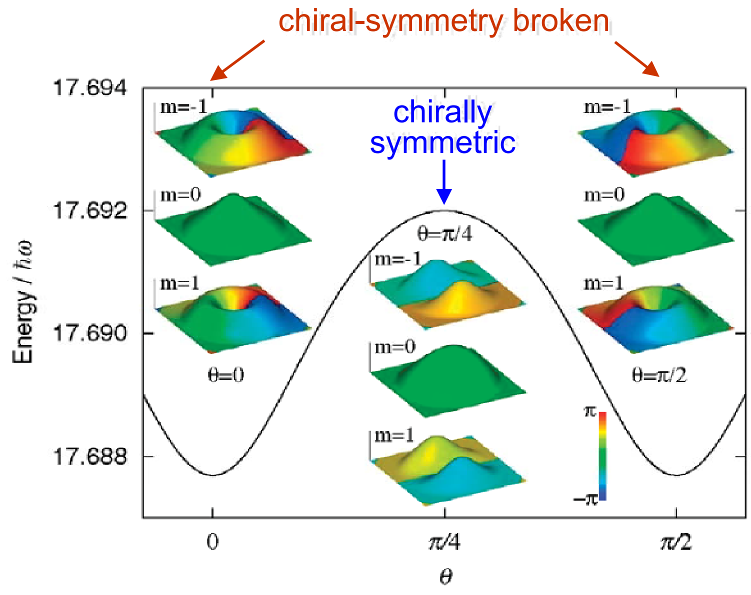

Chiral Symmetry Breaking in a Ferromagnetic BEC

Time development of orbital AM of $m = -1$ component

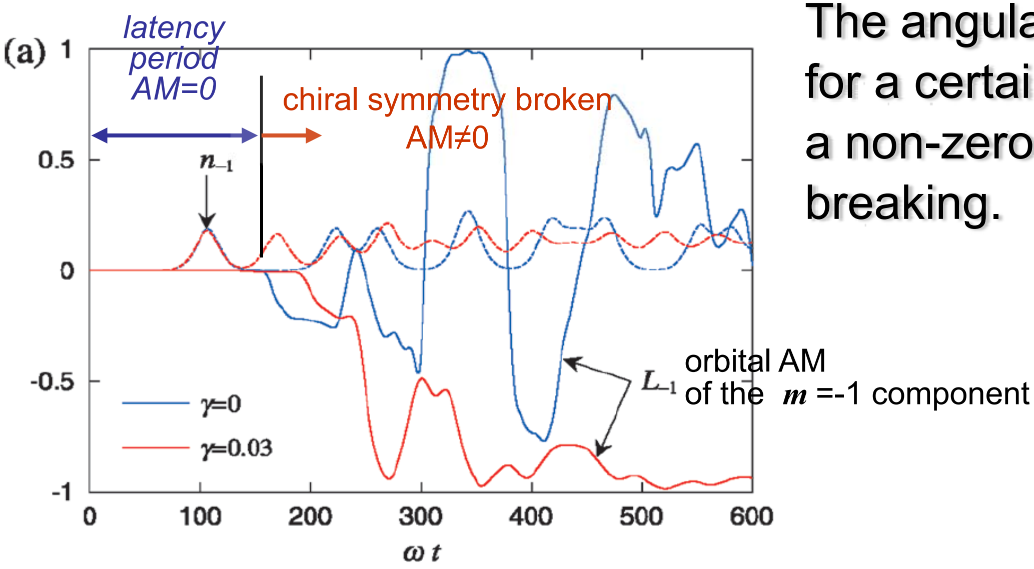

The angular momentum remains zero for a certain latency period and then acquires a non-zero value due to the chiral symmetry breaking.

Chiral Symmetry Breaking in a Ferromagnetic BEC

Time development of orbital AM $m = -1$ component

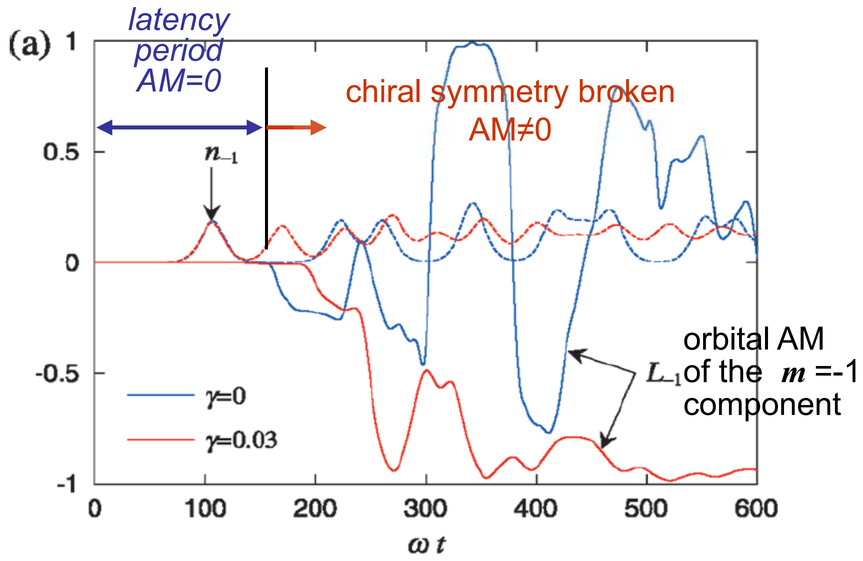

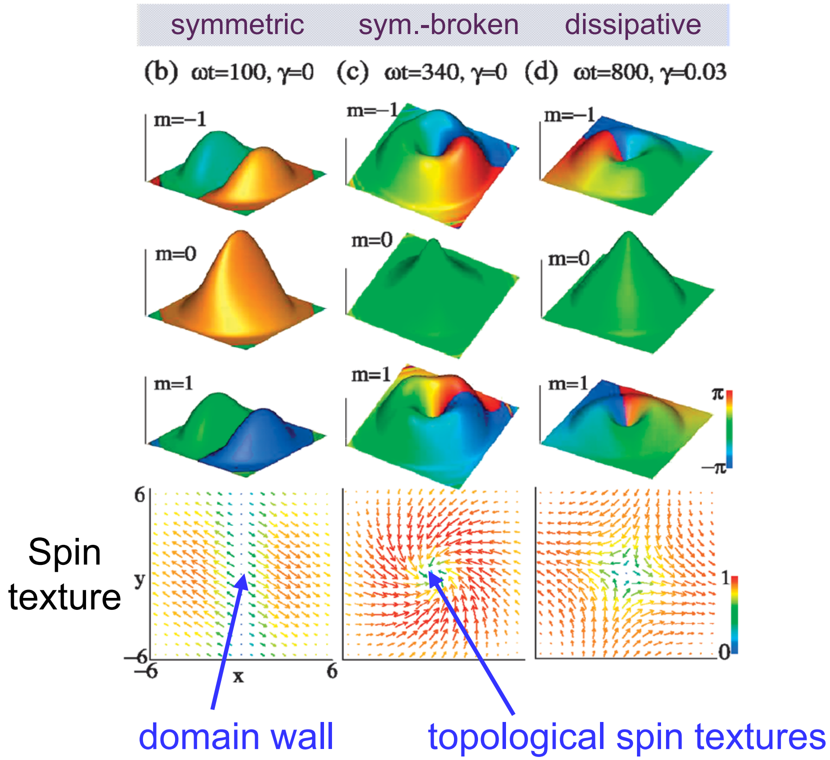

The chirally symmetric state has a domain wall which costs the ferromagnetic energy. The chiral-symmetry-broken state circumvents this energy cost by developing topological spin textures.

Prediction observed by the Berkeley group

L. E. Sadler, et al., Nature **443**, 312 (2006)

Initial conditions: all atoms in the *m*=0 state.

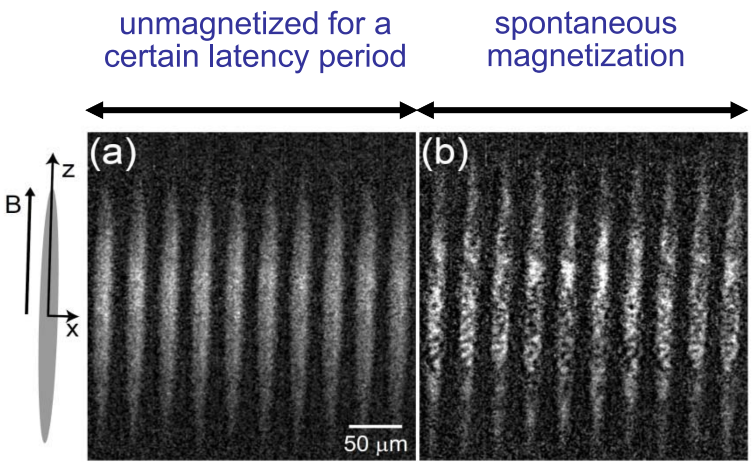

FIG. 1: Direct imaging of inhomogeneous spontaneous magnetization of a spinor BEC. Transverse imaging sequences (first 10 of 24 frames taken) are shown (a) for a single condensate probed at $T_{\mathrm{hold}} = 36$ ms and (b) for a different condensate at $T_{\mathrm{hold}} = 216$ ms. Shortly after the quench, the system remains in the unmagnetized $|m_z = 0\rangle$ state, showing neither short-range spatial nor temporal variation (i.e. between frames). In contrast, condensates at longer times are spatially inhomogeneous and display spontaneous Larmor precession as indicated by the cyclical variation of signal strength vs. frame number. Orientations of axes and of the magnetic field are shown at left.

← snapshots of the transverse magnetization of an elongated BEC

The system remained unmagnetized for a certain latency period before magnetization developed spontaneously.

Prediction observed by the Berkeley group

L. E. Sadler, et al., Nature **443**, 312 (2006)

Initial conditions: all atoms in the $m=0$ state.

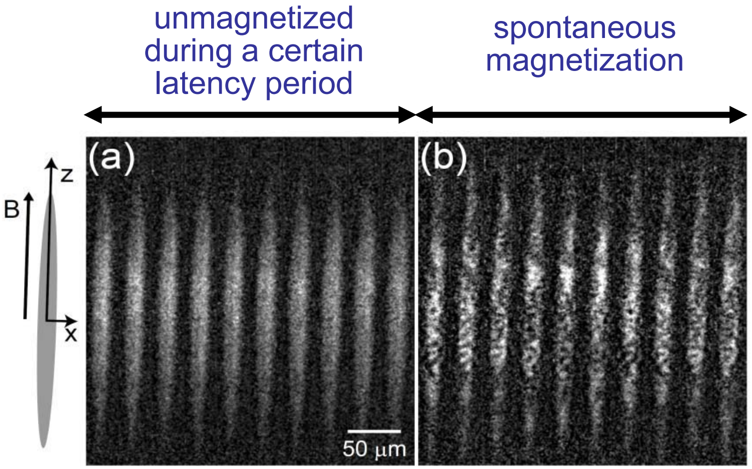

FIG. 1: Direct imaging of inhomogeneous spontaneous magnetization of a spinor BEC. Transverse imaging sequences (first 10 of 24 frames taken) are shown (a) for a single condensate probed at $T_{\text{hold}} = 36$ ms and (b) for a different condensate at $T_{\text{hold}} = 216$ ms. Shortly after the quench, the system remains in the unmagnetized $|m_z = 0\rangle$ state, showing neither short-range spatial nor temporal variation (i.e. between frames). In contrast, condensates at longer times are spatially inhomogeneous and display spontaneous Larmor precession as indicated by the cyclical variation of signal strength vs. frame number. Orientations of axes and of the magnetic field are shown at left.

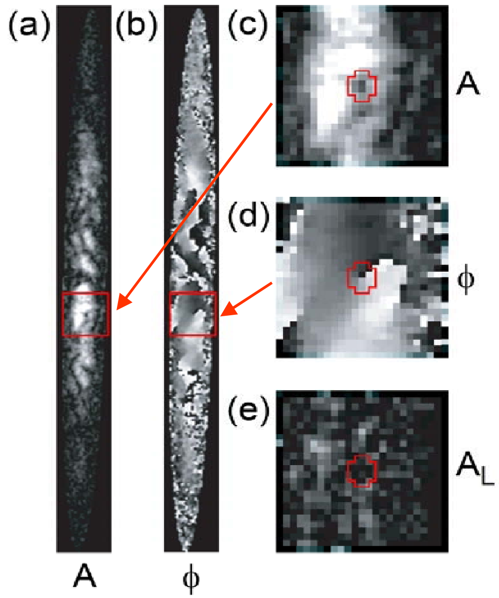

vortex of the $m=\pm 1$ components with its core filled wit the $m=0$ component

↓

This polar-core spin vortex corresponds to our chiral-symmetry broken state.

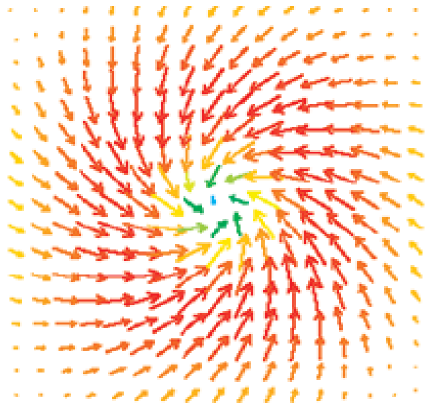

chiral-symmetry broken states

H. Saito, Y. Kawaguchi, and M.U., Phys. Rev. Lett. 96, 065302 (2006)

Formation Dynamics of Spin Vortices

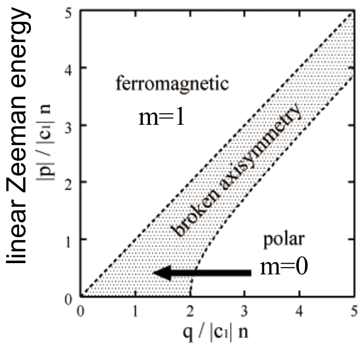

quadratic Zeeman energy

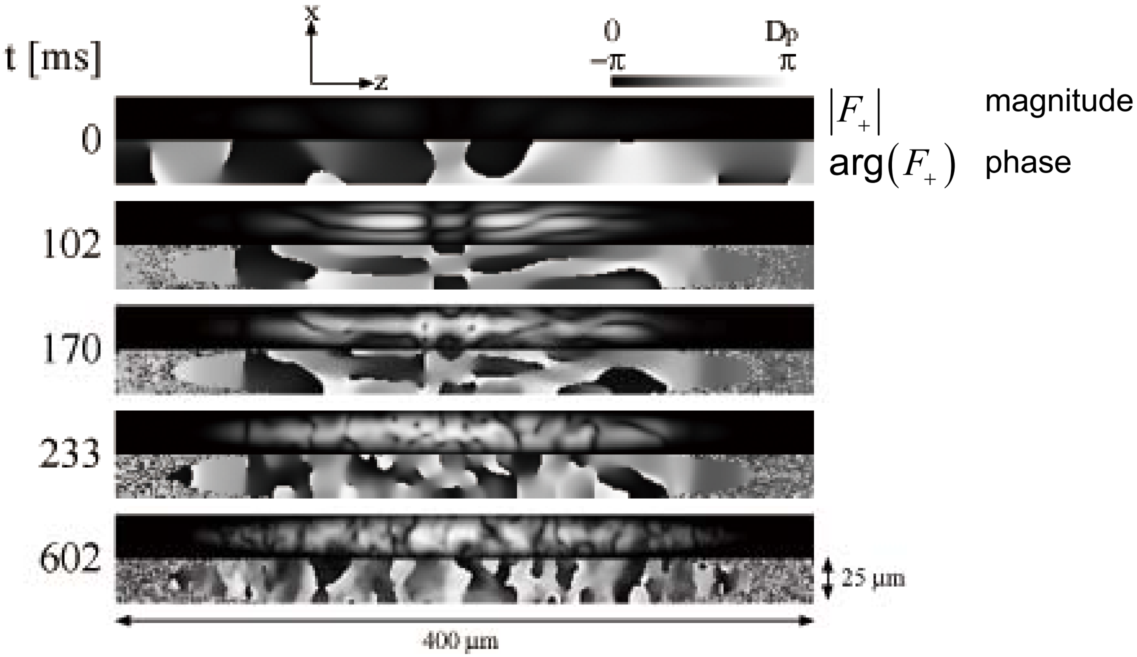

FIG. 6: Magnitude and direction of the spin for the initial condition given in Eq. (28) with $\lambda_{\mathrm{cutoff}} = 60\ \mu$m.

H.Saito, Y.Kawaguchi, and M.U., PRA **75**, 013602 (2007)

Minute fluctuations (quantum, thermal, etc.) at the moment of defect nucleations are amplified to yield observable magnetic domain structures.

Spin correlations give us information about the nature of initial noise.

A New Testing Ground for Kibble-Zurek Mechanism

Basic idea: spontaneous symmetry breaking at causally disconnected places generates topological defects (singularities) where the order parameter does not connect smoothly.

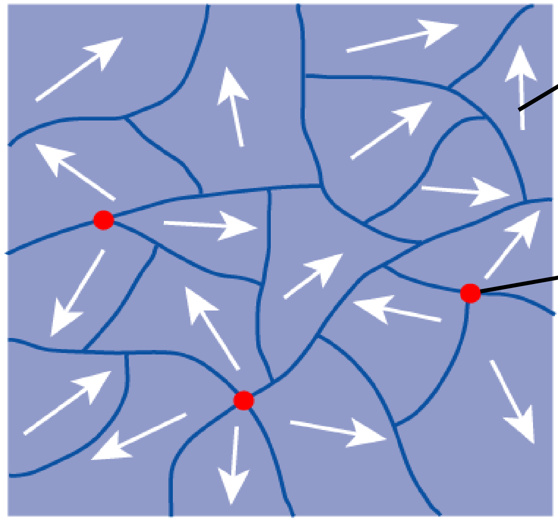

Order parameter

Superfluid phase
magnetization

Topological defects

vortices

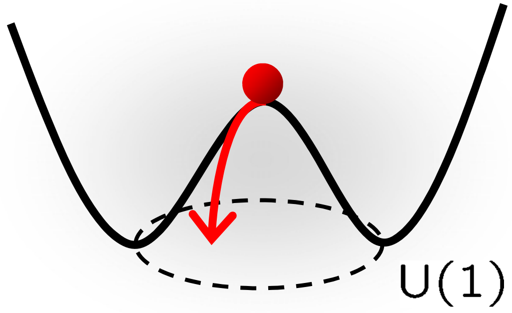

Cosmology, Superfluid He → Cold Atoms

T. W. Kibble, J. Phys. A **9**, 1387 (1976)
W. H. Zurek, Nature **317**, 505 (1985)

Detailed comparison between theory and experiments are feasible.

Spin Vortex Formation in a Quenched BEC

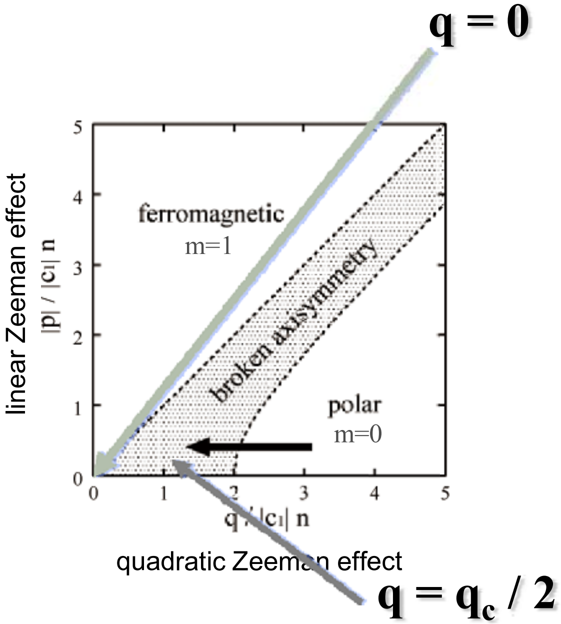

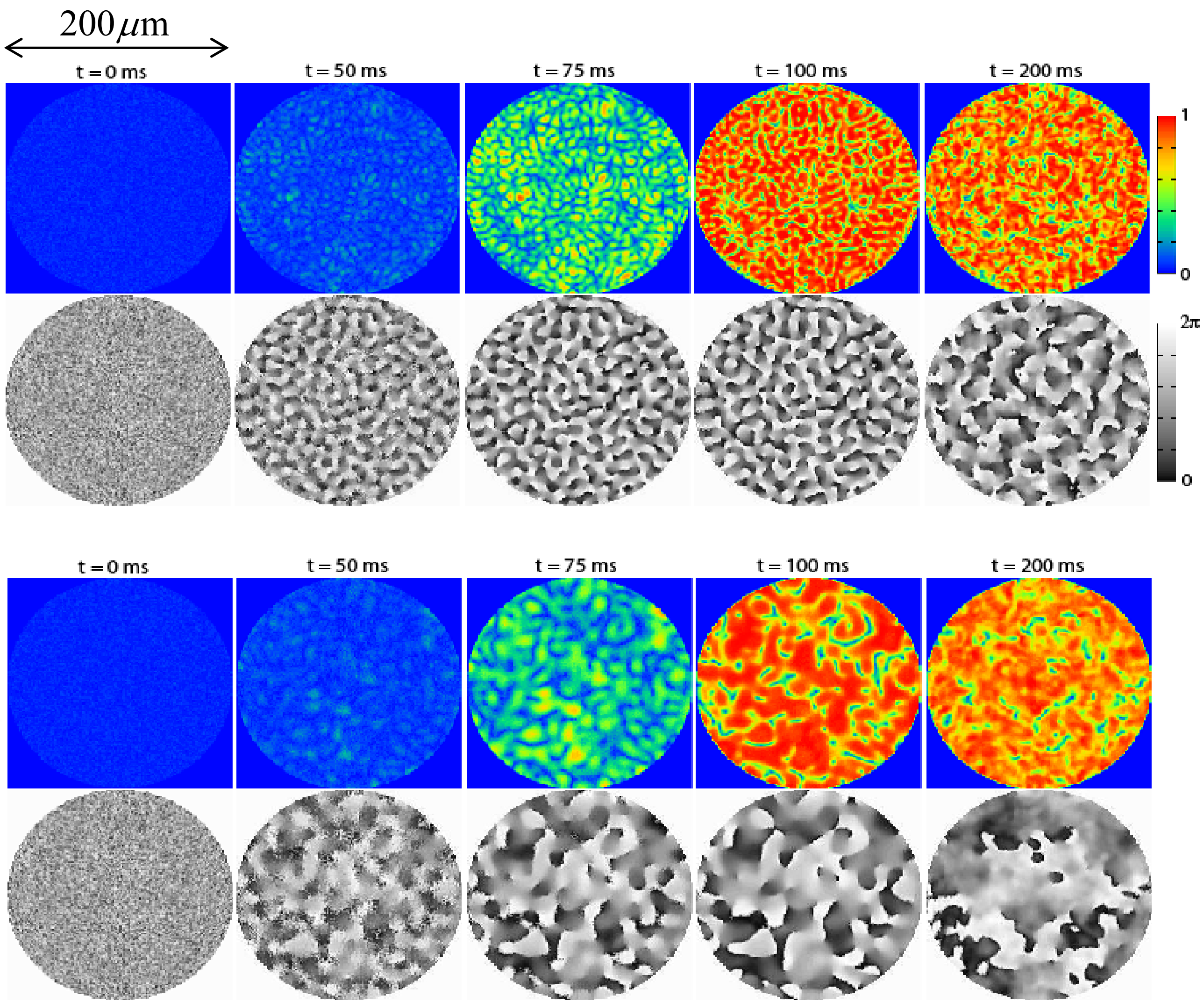

H. Saito, Y. Kawaguchi, and MU, to be published in PRA (cond-mat/0704.1377)

Winding Number and Scaling Law: Prediction

spin winding number

$$w = \frac{1}{2\pi} \oint d\mathbf{r} \bullet \frac{1}{2i\left|F_+\right|^2}\left(F_- \nabla F_+ - F_+ \nabla F_-\right)$$

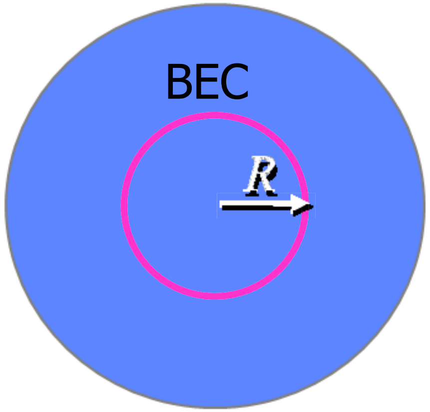

KZ

winding number

$$\propto \sqrt{R}$$

R=linear dimension of the system

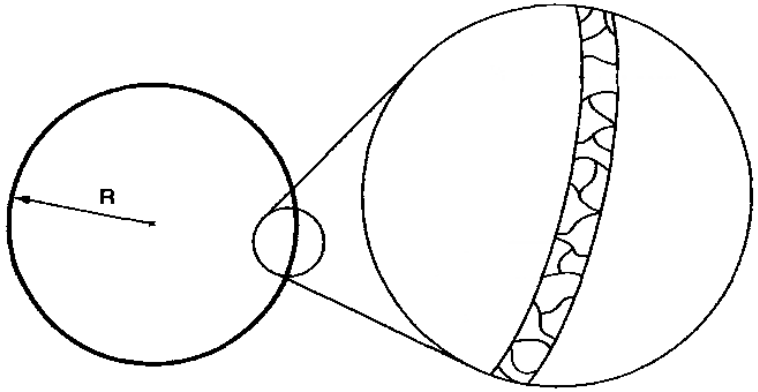

Zurek, Nature **317**, 505 (1985)

Winding Number and Scaling Law: Numerical Results

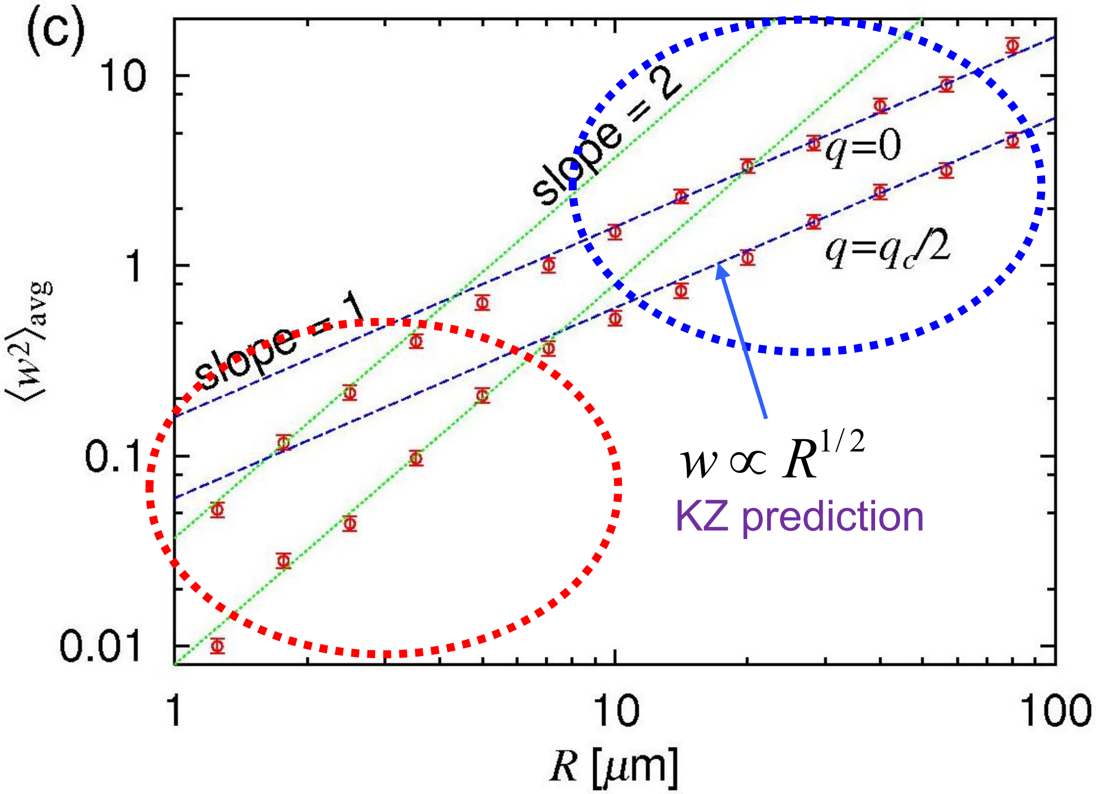

$w \propto R^{1/2}$ for large R

$w \propto R^{1}$ for small R $\qquad R \ll$ vortex spacing

H. Saito, Y. Kawaguchi, and MU, to be published in PRA
(cond-mat/0704.1377)

Summary

--- A rich variety of spinor BEC ---

New Quantum Phases, Magnetism, and Symmetry Breaking

- Spin-1 polar BEC: 1/2 vortex
- Spin-2 cyclic BEC: 1/3 vortex
- Spin-2 polar BEC: Meissner-like effect
- Topological defects: spin vortex with broken chiral symmetry
  Kibble-Zurek mechanism